SCIENTIFIC REPORTS

OPEN

SUBJECT AREAS:
SENSORS
ELECTRONIC MATERIALS AND DEVICES
SURFACE CHEMISTRY
APPLIED PHYSICS

Received
30 September 2011

Accepted
4 November 2011

Published
23 November 2011

Correspondence and requests for materials should be addressed to H.M.C. (cheng@imr.ac.cn) or N.K. (koratn@rpi.edu)

* These authors contributed equally to this work.

High Sensitivity Gas Detection Using a Macroscopic Three-Dimensional Graphene Foam Network

Fazel Yavari[1]*, Zongping Chen[2]*, Abhay V. Thomas[1], Wencai Ren[2], Hui-Ming Cheng[2] & Nikhil Koratkar[1,3]

[1]Department of Mechanical, Aerospace and Nuclear Engineering, Rensselaer Polytechnic Institute, 110 8th Street, Troy, New York 12180-3590, USA, [2]Shenyang National Laboratory for Materials Science, Institute of Metal Research, Chinese Academy of Sciences, Shenyang 110016, China, [3]Department of Materials Science and Engineering, Rensselaer Polytechnic Institute, 110 8th Street, Troy, New York 12180-3590, USA.

Nanostructures are known to be exquisitely sensitive to the chemical environment and offer ultra-high sensitivity for gas-sensing. However, the fabrication and operation of devices that use individual nanostructures for sensing is complex, expensive and suffers from poor reliability due to contamination and large variability from sample-to-sample. By contrast, conventional solid-state and conducting-polymer sensors offer excellent reliability but suffer from reduced sensitivity at room-temperature. Here we report a macro graphene foam-like three-dimensional network which combines the best of both worlds. The walls of the foam are comprised of few-layer graphene sheets resulting in high sensitivity; we demonstrate parts-per-million level detection of NH_3 and NO_2 in air at room-temperature. Further, the foam is a mechanically robust and flexible macro-scale network that is easy to contact (without Lithography) and can rival the durability and affordability of traditional sensors. Moreover, Joule-heating expels chemisorbed molecules from the foam's surface leading to fully-reversible and low-power operation.

Nanoscale structures such as carbon nanotubes[1–3] and graphene[4–5] have been considered as candidates for chemical sensing. Such sensors are attractive for "on-site" monitoring and can be used by emergency rescue crews or first responders for monitoring gas purity, air quality, and sensing potentially dangerous leaks. The Dai and Zettl groups first showed[1–2] that the electrical conductance of semi-conducting single-walled carbon nanotubes (SWNTs) changes sensitively at room temperature on exposure to several gases due to charge transfer between adsorbed gas molecules and nanotubes. For example, SWNTs are found to exhibit large increase in conductivity on exposure to oxygen[1]. Similarly hole doped (p-type) SWNTs exhibit three orders of magnitude increase in conductance[2] on exposure to 200 parts-per-million (ppm) of NO_2. On exposure to 1% (10,000 ppm) NH_3 flow, the same nanotubes exhibited a two orders of magnitude decrease in conductance[2]. Since O_2 and NO_2 are strong oxidizing agents, they attract electrons from the p-type SWNT, thereby increasing the number of conducting holes. This hole (or p-type doping) shifts the Fermi level closer to the valence band causing increase in conductance. On the other hand, reducing agents such as NH_3 that inject electrons into p-type SWNT reduce the number of holes, leading to reduced conductance.

Individual graphene sheets[4–5] can also be used to construct ultra-sensitive gas sensor devices. Graphene exhibits an exceptional band structure which contains conduction and valence bands with quasi-linear dispersion that touch at the Brillouin zone corners to form a zero gap semiconductor. Due to these properties as well as ultra-high surface area provided by graphene, its electronic properties show strong dependence to surface absorbents, including gas molecules, that can alter the carrier density of graphene. It has been shown that graphene and reduced graphene oxide respond sensitively to the adsorption of trace amounts of different gases including NH_3, NO_2, H_2O, Cl_2 and CO[6–12]. The very high sensitivity of graphene is also due in-part to its inherently low electrical noise[4–5] at room temperature which arises from its unique two-dimensional crystal lattice. Despite the outstanding potential of graphene and carbon nanotubes as gas sensors, the path of these devices towards commercialization is hindered by the complexity and cost of the fabrication process, durability/robustness of the sensor devices and large variability from sample-to-sample. For example, devices utilizing individual SWNT or graphene require patterning and subsequent electrode attachment using lithography[6–7, 12–16] which increases the cost. Since individual SWNT or graphene elements are exquisitely sensitive to the chemical environment, they are easily susceptible to extraneous factors. This can affect the repeatability and reliability of the device performance.

Besides, such devices can be fragile and difficult to repair and maintain in the field. Here we report a mechanically robust and flexible 3D macro graphene foam (GF) network that offers the durability and affordability of macro sensors coupled with the very high sensitivity of a nanosensor device. We recently reported[17] the development of such a free-standing continuous graphene-based network structure for flexible electronics applications. Here we show that such an inexpensive and simple GF device can also be utilized for chemical sensing with high sensitivity and reversibility.

Results

To fabricate the GF, a scaffold of porous nickel foam is used as a template for the deposition of graphene.[17] Using chemical vapor depositon (CVD)[18], carbon atoms are deposited on the nickel foam using CH4 decomposition at ~1000° C under ambient pressure. The nickel scaffold is then removed using chemical etching by a hot HCl (or $FeCl_3$) solution. To maintain the integrity of the foam during the etching of the Ni and to prevent it from collapsing, a thin layer of poly(methyl methacrylate) (PMMA) is also deposited on the surface of the graphene formed on the nickel foam. In the final step the PMMA layer is dissolved by hot acetone. What remains is a continuous 3D network of graphene formed as a free-standing macroscopic structure with extremely thin interconnected sheets of graphene (Figure 1a–b). More details of the fabrication process of GF can be found in our previous work.[17] The GF resembles the interconnected 3D scaffold structure of the initial nickel foam template. The graphene films in GF grow on the entire surface of the nickel foam scaffold and hence they are interconnected into each other and there is no interface or physical breaks in the network. Importantly, graphene films formed on the different surfaces of the nickel foam are well separated from each other, providing more adsorption sites for gas molecules. The GF is also very porous, flexible and light-weight and has a very high specific surface area of ~850 m^2/g determined by standard BET nitrogen cryosorption characterization. The GF fabricated using a CH_4 concentration of 0.7 vol% which was used in the present study has an extremely low density of ~5 mg/cm^{-3}, corresponding to a very high porosity of ~99.7%.[17] The thickness of the GF sample used in our study was ~0.5 mm. Raman spectroscopy analysis of the foam (Figure 1c) indicates that the walls of the GF are comprised of monolayer to few-layer graphene sheets. This is consistent with the specific surface area of ~850 m^2/g measured for the GF. The Raman spectra (Figure 1c) also show a strongly-suppressed defect-related D band, which confirms the overall high quality of the graphene in the foam.

In GF charge carriers can move rapidly with a small resistance through the continuous and interconnected network of high quality CVD-grown graphene building blocks, resulting in high electrical conductivity (~10 S/cm). The operational mechanism of the GF sensors presented in this work is based on changes in their electrical conductivity, due to charge transfer induced by the adsorption of gas molecules acting as donors or acceptors[4–5] on to the foam's surface. To measure the change in conductivity of GF by adsorption of gases, a four-probe resistance measurement technique was used (see Methods). Note that no lithographic patterning or manipulation of the sample is necessary; the flexible and robust macro-scale GF can be used directly in the as-produced condition. Proof-of-concept gas sensing experiments are performed using trace amounts of NH_3 and NO_2 in mixtures with air at room temperature and atmospheric pressure. The temperature dependence of desorption of gas species is also studied using a hot plate with a temperature sensor. Heating increases the reversibility of the device and also accelerates the response rates. Another advantage of the robust GF device is that Joule heating can be conveniently used to locally heat the foam thereby achieving excellent reversibility of the sensor response. All of the data presented in this paper are obtained using one device, but similar response was reproduced in three other devices.

Discussion

To demonstrate the proof-of-concept, we chose ammonia (NH_3) as a test gas. Ammonium nitrate present in explosives is known to gradually decompose and release trace amounts of NH_3 which if detected would indicate presence of an explosive. NH_3, a toxic gas, is also used in a variety of industrial and medical processes and therefore it becomes important to monitor for NH_3 leaks. The GF device was

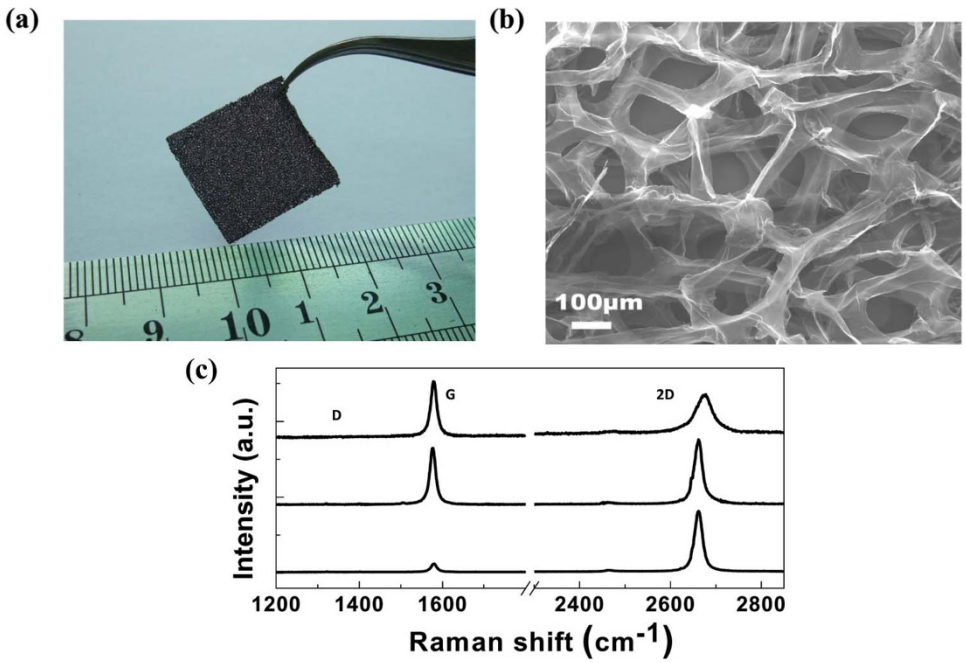

Figure 1 | Characterization of the GF structure. (a) Photograph and (b) scanning electron micrograph of the microporous GF structure showing a continuous network of 3D interconnected graphene sheets that comprise the walls of the foam-like structure. The robust and flexible GF strips can be easily handled and manipulated. Electrical contacts to the macro-scale GF can be established without the need for lithography. (c) Typical Raman spectra obtained at various locations on the GF indicating that the foam walls are comprised of mono to few-layer graphene.

placed in an environmental chamber with electrical feed-through, and air was pumped out of the chamber to establish a high vacuum ($\sim 10^{-6}$ torr). Next NH_3 gas pre-mixed with air at the appropriate concentration was released into the chamber. We exposed the GF device for ~800 seconds to ~1000 parts-per-million (ppm) of NH_3 diluted in air at atmospheric pressure and room temperature (~300 K). The time evolution of the change in resistance due to adsorption of gas molecules is shown in Figure 2a. NH_3 appears to cause a decrease in the number of charge carriers in the foam resulting in an increase in resistance. Graphene under ambient conditions has been observed to display p-type behavior[19] due to the electron withdrawing nature of adsorbed water or oxygen containing moeties which induce a holelike carrier concentration. NH_3 is a reducing agent with a lone electron pair that can be donated to the p-type GF thereby reducing the conductance. This change in resistance normalized by the initial resistance ($\Delta R/R$) is defined as the sensitivity of the GF and it is ~30% for the case of ~1000 ppm of ammonia. The resistance of the GF reaches ~90% of its steady state value after ~500 seconds. Steady state is defined as the condition when the resistance value shows <1% change over a ~60 second time interval. To study the reversibility of the device, the gas input is closed and the NH_3-dosed device was exposed to vacuum desorption conditions for another ~800 seconds. As Figure 2a shows the resistance of the sample does not return to the initial value even after prolonged exposure to vacuum and ~13.8% of the response is not recoverable. This shows that the desorption process is much slower than the adsorption process, likely due to chemisorption of NH_3 to the graphene surface. Purging the chamber with pure air for ~800 seconds also did not lead to full reversibility of the sensor response.

To stimulate the desorption process in GF, a heater was placed under the GF device and a temperature sensor was used to measure the foam temperature. Figure 2b shows the change in resistance as a function of time when a heater is used. The GF temperature is also measured and illustrated in the graph as a function of time. As seen in this graph, the heating significantly accelerates the desorption process, by exciting the molecules vibrationally so that they enter a repulsive state[20]. After the heater is turned off, the $\Delta R/R$ of the GF equilibriates close to the original value, showing good reversibility. Even though the use of an external heater helps to achieve complete desorption in a shorter time, it will make the device bulky and complicated. A much more elegant approach is to use the Joule heating effect to generate the heat locally within the sample. For calibration purpose, the GF sample was heated in the 300–450 K temperature range using the external heater under vacuum ($\sim 10^{-6}$ torr) and the reduction in resistance was measured as a function of temperature (see Supplementary Fig. S1). The GF displays a semi-conducting behavior with a negative coefficient of thermal resistivity of about ~0.00125 Ω/K. Next, a controlled Joule heating current (I) was applied to resistively heat the GF sample. Increasing the current also decreases the values of resistance (Supplementary Fig. S2), confirming that there is a Joule heating effect. From Figures S1 and S2 (Supplementary Section), one can associate each value of current (I) to a temperature (T), for example, to achieve ~400 K in the GF, a current of ~125 mA is required. In figure 2c, we show the results of an experiment performed with Joule heating (I=125 mA) used to accelerate the desorption process. As seen in this graph, the adsorption process is fully reversible and the desorption time is almost as short as the adsorption time. Note that the electrical current range for sensing signals is ~1 mA, while the Joule heating current as previously discussed is of the order of ~100 mA.

Figure 3a shows the reversibility of the sensor over several cycles with Joule heating during the desorption step. Figure 3b shows the normalized change in GF resistance ($\Delta R/R$) as function of time for different concentrations of NH_3 ranging from 1000 ppm (0.1%) to 20 ppm (0.002%). All tests are performed at atmospheric pressure and room temperature with Joule heating used during desorption.

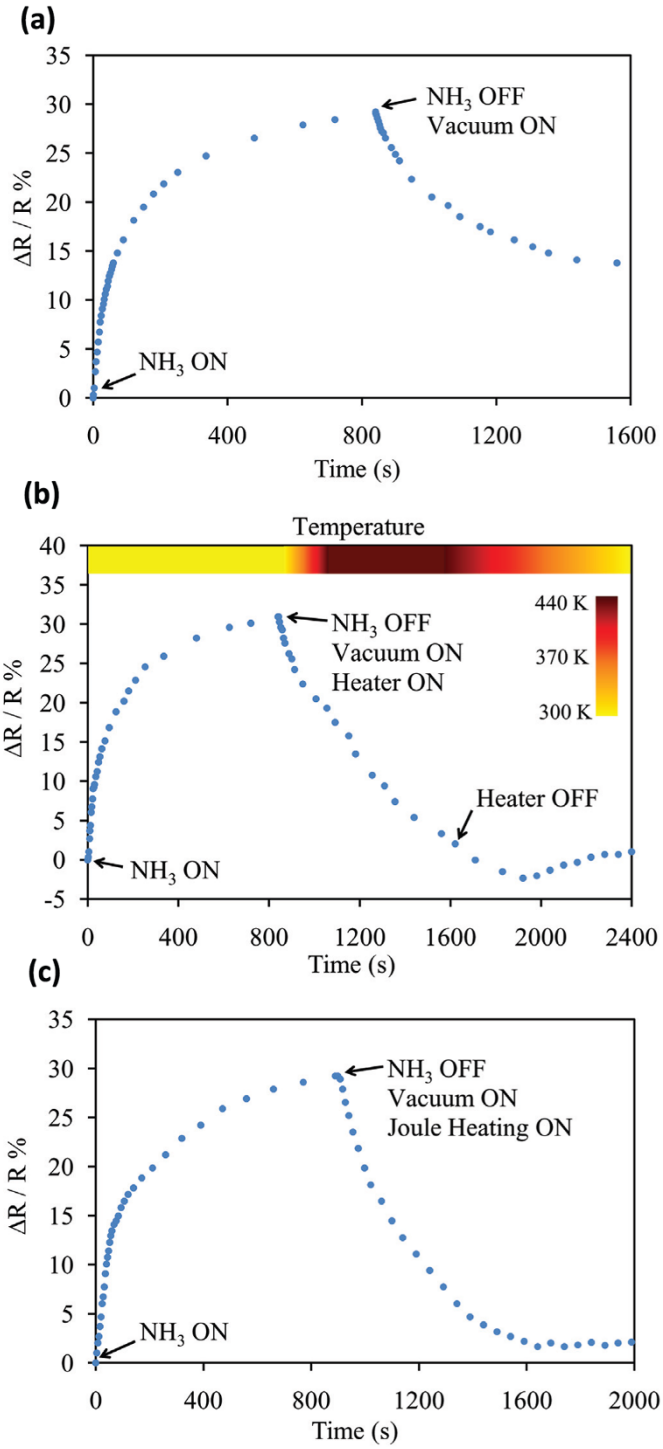

Figure 2 | GF sensor response. Change in the normalized resistance of the GF as a function of time during adsorption of ~1000 ppm of NH_3 and desorption using (a) room temperature degassing and (b) high temperature degassing. The color bar at the top of the graph in (b) shows the change in temperature as a function of time. (c) Corresponding adsorption and desorption response obtained by using Joule heating of the sample during the desorption step. The control current supplied to the GF to heat it to ~400 K is ~125 mA.

The $\Delta R/R$ of the GF device decreases from ~30% for 1000 ppm to ~5% for 20 ppm of NH_3 which is well above the background noise level. Typical NH_3 gas sensors operate in the 1 to 0.1% range of NH_3 concentrations in air. For example in Ref. 2, the individual SWNT device was used to detect ~0.1% (i.e. 1000 ppm) of NH_3 in air. Here

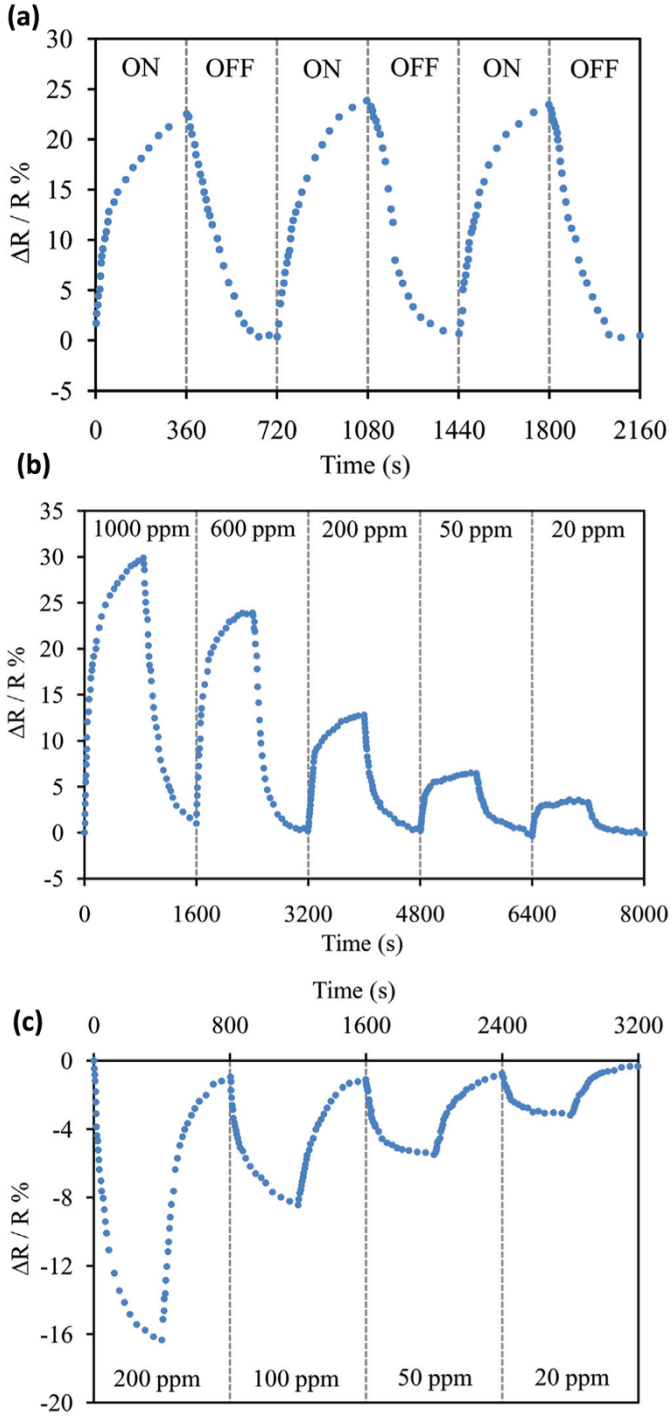

Figure 3 | Reversibility and sensitivity of the GF sensor for detection of NH_3 and NO_2. (a) Normalized change in electrical resistance of the GF as a function of time for detection of ~1000 ppm of NH_3 in three cycles. With Joule heating during the desorption step, the GF sensor exhibits a fully reversible response. (b) Normalized resistance change vs. time for different concentrations of NH_3 in air. The adsorption step is performed at room temperature, while Joule heating to ~400 K is used during desorption. (c) Corresponding normalized resistance change vs. time for different concentrations of NO_2 in air.

we detect NH_3 concentrations that are nearly two orders of magnitude lower (~20 ppm) using a robust and inexpensive GF device that is also very easy to handle and use. Commercially available conducting polymer sensors[21] undergo ~30% resistance change in 5–10 minutes when exposed to ~1% (10,000 ppm) of NH_3 at room temperature. By contrast, the GF sensor undergoes ~30% resistance change at room temperature at an order of magnitude lower NH_3 concentration of ~1000 ppm (Fig. 3b). Other viable NH_3 sensor technologies such as metal oxide sensors require high temperature operation (between 300–500° C) for adequate sensitivity[22]. These devices suffer from high power consumption due to their high working temperatures. Therefore the ability to detect gas species at room temperatures with high sensitivity and low production cost is of great practical relevance.

In addition to NH_3 we also explored the effectiveness of the GF sensor for NO_2 detection at room temperature and atmospheric pressure. Explosives such as nitrocellulose gradually degrade and a byproduct is known to be NO_2 gas, which provides a fingerprint for its detection. Monitoring environmental pollution effects related to combustion or automotive emissions also requires NO_2 detection in real-time. Figure 3c shows the normalized change in the GF resistance ($\Delta R/R$) as a function of time for different concentrations of NO_2 ranging from 200 ppm down to 20 ppm. NO_2 appears to act as a p-type dopant for the GF resulting in a decrease in the resistance. The $\Delta R/R$ of the GF device decreases from ~16% for 200 ppm to ~4% for 20 ppm of NO_2. As before Joule heating of the sample to ~400 K using 125 mA control current was effective in achieving full reversibility of the sensor response. Compared to this commercial polypyrole conducting polymer sensors can detect ~0.1% (1000 ppm) of NO_2 by an ~10% resistance change in ~5–10 minutes at room temperature[21]. The GF sensor shows a comparable resistance change at room temperature at an order of magnitude lower NO_2 concentration (Fig. 3c). Other commercial NO_2 detectors (e.g. metal oxide sensors such as Cd-doped SnO_2) are limited by high power consumption requirements since they require elevated temperature operation (>200° C) for adequate sensitivity[22–23].

We have demonstrated the effectiveness of macroscopic and continuous graphene foam-like 3D networks for the high sensitivity detection of NH_3 and NO_2 at room temperature and atmospheric pressure. Large sheets (several tens of inches in dimensions) of GF can be synthesized using thermal CVD and then cut into tens or even hundreds of smaller foams which can be directly used in the as-produced state. The cost and complexity of sensor fabrication, maintenance and operation are therefore likely to be lower as compared to individually deposited or cleaved graphene sheets that must be patterned lithographically to establish electrical contacts. By contrast, the GF device is mechanically robust, flexible and can be handled easily. Contacts to the macroscale foams can be established by simply attaching wires using silver epoxy. Importantly, the GF structures also offer high sensitivity of gas detection in the ppm range. Since the walls of the foam are comprised on average of only few-layer graphene films, charge carrier transport through the foam is highly sensitive to the adsorption/desorption of gas species. The very large porosity of the foam also makes it possible for gas molecules to infiltrate uniformly into the entire structure resulting in high sensitivity and stable operation of the device. Moreover, Joule-heating can be used to expel chemisorbed gas molecules on the GF leading to fully reversible operation. The simple, low-cost sensors described here could be deployed for a variety of applications, such as environmental monitoring, sensing in chemical processing plants, and gas detection for counter-terrorism.

Methods

Graphene Foam (GF) Synthesis: To fabricate the GF, a scaffold of porous nickel foam is used as a template for the deposition of graphene. Chemical vapor deposition (CVD) is used to deposit carbon atoms on the nickel foam using CH_4 decomposition at ~1000°C under ambient pressure. The nickel scaffold is then removed using chemical etching by a hot HCl (or $FeCl_3$) solution. To maintain the integrity of the foam during the etching of the Ni and to prevent it from collapsing, a thin layer of poly(methyl methacrylate) (PMMA) is also deposited on the surface of the graphene formed on the nickel foam. In the final step the PMMA layer is dissolved by hot acetone resulting in a free-standing three-dimensional graphene network structure. Additional details regarding the process are provided in Reference 17.

Electrical Conductivity Measurements: The foam is cut into small pieces of ~2 mm in width and ~10 mm in length and then connected to a chip carrier using thin copper wires at four different points. The contacts to the wires are simply made using conductive silver epoxy (EJ-2189 two part kit from EPOXY Technology) on the foam side, and wire bonding on the chip carrier side. The four leads of the chip carrier are then connected to a current source and voltmeter to conduct the four-probe measurement test using LabView. The four-probe method is important in that it eliminates the effect of contact resistances. In such a configuration, the sensor response depends only on the changes in resistance of the graphene sheet and spurious effects related to the role of the electrical contacts are removed.

1. Collins, P., Bradley, K., Ishigami, M. & Zettl, A. Extreme oxygen sensitivity of electronic properties of carbon nanotubes. *Science* **287**, 1801–1804 (2000).
2. Kong, J. *et al*. Nanotube molecular wires as chemical sensors. *Science* **287**, 622–625 (2000).
3. Ong, K.-G., Zeng, K., Grimes, C. A wireless, passive carbon nanotube-based gas sensor. *IEEE Sensors* **2**, 82–88 (2002).
4. Schedin, F. *et al*. Detection of individual gas molecules adsorbed on graphene. *Nature Materials* **6**, 652–655 (2007).
5. Leenaerts, O., Partoens, B., Peeters, F. M. Adsorption of H_2O, NH_3, CO, NO_2, and NO on graphene: A first-principles study. *Physical Review B* **77**, 125416 (2008).
6. Yavari, F. *et al*. Tunable bandgap in graphene by the controlled adsorption of water molecules. *Small* **6**, 2535–2538 (2010).
7. Dan, Y. P., Lu, Y., Kybert, N. J., Luo, Z. T. & Johnson, A. T. C. Intrinsic response of graphene vapor sensors. *Nano Letters* **9**, 1472–1475 (2009).
8. Wu, W. *et al*. Wafer-scale synthesis of graphene by chemical vapor deposition and its application in gas sensing. *Sensors and Actuators B: Chemical* **150**, 296–300 (2010).
9. Fowler, J. D., Allen, M. J., Tung, V. C., Yang, Y., Kaner, R. B., Weiller, B. H. Practical chemical sensors from chemically derived graphene. *ACS Nano* **3**, 301–306 (2009).
10. Lu, G. H. *et al*. Toward practical gas sensing with highly reduced graphene oxide: a new signal processing method to circumvent run-to-run and device-to-device variations. *ACS Nano* **5**, 1154–1164 (2011).
11. Lu, G. H., Ocola, L. E., Chen, J. H. Gas detection using low-temperature reduced graphene oxide sheets. *Applied Physics Letters* **94**, 3, 08311 (2009).
12. Robinson, J. T., Perkins, F. K., Snow, E. S., Wei, Z. Q., Sheehan, P. E. Reduced graphene oxide molecular sensors. *Nano Letters* **8**, 3137–3140 (2008).
13. Zhang, Y. B., Tan, Y. W., Stormer, H. L., Kim, P. Experimental observation of the quantum Hall effect and Berry's phase in graphene. *Nature* **438**, 201–204 (2005).
14. Du, X., Skachko, I., Barker, A., Andrei, E. Y. Approaching ballistic transport in suspended graphene. *Nature Nanotechnology* **3**, 491–495 (2008).
15. Wei, B., Vajtai, R., Ajayan, P. M. Reliability and current carrying capacity of carbon nanotubes. *Appl. Phys. Lett.* **79**, 1172 (2001).
16. Pati, R., Zhang, Y., Nayak, S., Ajayan, P. M. Effect of H_2O adsorption on electron transport in a carbon nanotube. *Appl. Phys. Lett.* **81**, 2638 (2002).
17. Chen, Z. P., Ren, W. C., Gao, L. B., Liu, B. L., Pei, S. F., Cheng, H. M. Three-dimensional flexible and conductive interconnected graphene networks grown by chemical vapour deposition. *Nature Materials* **10**, 424–428 (2011).
18. Li, X. S. *et al*. Large-area synthesis of high-quality and uniform graphene films on copper foils. *Science* **324**, 1312–1314 (2009).
19. J. Moser, A. Verdaguer, D. Jimenez, A. Barreiro, A. Bachtold, The environment of graphene probed by electrostatic force microscopy. *Appl. Phys. Lett.* **92** (2008).
20. Yang, F., Taggart, D. K., Penner, R. M. Joule heating a palladium nanowire sensor for accelerated response and recovery to hydrogen gas. *Small* **6**, 1422–1429 (2010).
21. J. Miasik, A. Hooper, B. Tofield, Conducting polymer gas sensors *J. Chem. Soc. Faraday Trans. 1* **82**, 1117–1126 (1986).
22. Y. Shimizu, M. Egashira, Basic aspects and challenges of semiconductor gas sensors. *MRS Bull.* **24**, 18–24 (1999).
23. G. Sberveglieri, S. Groppelli, P. Nelli, Highly sensitive and selective NO_x and NO_2 sensor based on Cd-doped SnO_2 thin films. *Sens. Actuators B* **4**, 457–461 (1991).

Acknowledgements

N.K. acknowledges funding support from the Advanced Energy Consortium (AEC). H.M.C. acknowledges support from the National Science Foundation of China (Nos. 50921004, 50872136 and 50972147) and the Chinese Academy of Sciences (No. KJCX2-YW-231).

Author contributions

NK and HMC planned the experiments. ZC and WR fabricated the graphene foam. FY, AVT and NK performed the gas sensing experiments and processing of the data. All authors contributed to the discussion of the results. HMC and NK wrote the paper.

Additional information

Supplementary information accompanies this paper at http://www.nature.com/scientificreports

Competing financial interests: The authors declare no competing financial interests.

How to cite this article: Yavari, F. *et al*. High Sensitivity Gas Detection Using a Macroscopic Three-Dimensional Graphene Foam Network. *Sci. Rep.* **1**, 166; DOI:10.1038/srep00166 (2011).